Pharm Res (2014) 31:593–606
DOI 10.1007/s11095-013-1183-4

RESEARCH PAPER

Semi-mechanistic Modelling of the Analgesic Effect of Gabapentin in the Formalin-Induced Rat Model of Experimental Pain

A. Taneja • I. F. Troconiz • M. Danhof • O. Della Pasqua • on behalf of the neuropathic pain project of the PKPD modelling platform

Received: 3 March 2013 / Accepted: 9 August 2013 / Published online: 5 October 2013

ABSTRACT

Purpose The formalin-induced rat model of nociception involves moderate continuous pain. Formalin-induced pain results in a typical repetitive flinching behaviour, which displays a biphasic pattern characterised by peaks of pain. Here we described the time course of pain response and the analgesic effect of gabapentin using a semi-mechanistic modelling approach.

Methods Male Sprague-Dawley rats received gabapentin (10–100 mg/kg) or placebo 1 h prior to the formalin injection, as per standard protocol. A reduction in the frequency of the second peak of flinching was used as a behavioural measure of gabapentin-mediated anti-nociception. The flinching response was modelled using a mono-exponential function to characterise the first peak and an indirect response model with a time variant synthesis rate for the second. PKPD modelling was performed using a population approach in NONMEM v.7.1.2.

Results The time course of the biphasic response was adequately described by the proposed model, which included separate expressions for each phase. Gabapentin was found to reversibly decrease, but not suppress the flinching frequency of the second response peak only. The mean IC_{50} estimate was 7,510 ng/ml, with relative standard error (RSE%) of 40%.

Conclusions A compartmental, semi-mechanistic model provides the basis for further understanding of the formalin-induced flinching response and consequently to better characterisation of the properties of gabapentin, such as the potency in individual animals. Moreover, despite high exposure levels, model predictions show that gabapentin does not completely suppress behavioural response in the formalin-induced pain model.

KEY WORDS drug development · formalin-induced pain · gabapentin · neuropathic pain · pharmacokinetic-pharmacodynamic modelling

ABBREVIATIONS

CI	confidence interval
COX-2	cyclo-oxygenase 2
CV	coefficient of variation
GABA	γ-amino butyric acid
IIV	inter-individual variability
MED	median effective dose
MOFV	minimum objective function value
NK1	neuroenkephalin 1
NMDA	N-methyl *d*-aspartate
PKPD	pharmacokinetics and pharmacodynamics
RSE	relative standard error
VPC	visual predictive check

INTRODUCTION

Ideally, the evaluation of the efficacy of novel treatments for neuropathic pain should be based on pre-clinical models that mimic not only the symptoms of disease, but also consider the substrates underlying the pathophysiology of nociception in humans, i.e., show construct validity (1). Nevertheless, most

Electronic supplementary material The online version of this article (doi:10.1007/s11095-013-1183-4) contains supplementary material, which is available to authorized users.

A. Taneja · M. Danhof · O. Della Pasqua (✉)
Division of Pharmacology, Leiden Academic Centre for Drug Research
POBox 9502, 2300 RA, Leiden, The Netherlands
e-mail: odp72514@gsk.com

I. F. Troconiz
Department of Pharmacy and Pharmaceutical Technology
Faculty of Pharmacy, University of Navarra, Pamplona, Spain

O. Della Pasqua
Clinical Pharmacology Modelling & Simulation, GlaxoSmithKline
Uxbridge, Middlesex, UK

behavioural models of pain rely on withdrawal responses to evoked pain, which reflect sensory perception and consequently one's ability to discriminate its intensity, localisation and modality (2,3). As such, these measures ignore other features of human pain (4).

Regardless of the potential limitations mentioned above, the formalin induced pain (FIP) model is a well-accepted screening test. The method comprises moderate, continuous pain due to tissue injury following injection of formalin. In the FIP model, the observed behaviour in response to a painful stimulus, assessed as flinching frequency, is used as a measure of efficacy (2,5,6). More specifically, the response is described by a biphasic profile, which corresponds to the processes underlying peripheral and central sensitisation. In addition, this behaviour is thought to reflect both the sensory and emotional aspects of pain (7,8). From a mechanistic perspective, the presence of common elements of human pain behaviour in the FIP model makes it possibly one of the most predictive models among the available experimental models of acute pain. These properties have also made the FIP model an appealing tool for the screening of compounds showing potential central anti-nociceptive activity (6,9). In fact, various compounds have been found to affect flinching behaviour (e.g., indomethacin and Na^+ channel blockers), as assessed by the inhibition of the second pain peak (2,10).

In the current investigation, we evaluate the pharmacokinetic-pharmacodynamic (PKPD) properties of gabapentin in the FIP model. Gabapentin is believed to act via antagonism of voltage gated Ca^{++} channels in afferent neurons, thereby indirectly modulating GABA activity (11). It has been shown to affect the amplitude of the second pain peak, whilst leaving the other components of the pain response largely unaffected (12).

Despite the widespread use of gabapentin as a reference compound in preclinical models, no quantitative methods have been implemented so far that allow discrimination between pharmacological and biological system properties, and consequently provide a more consistent ranking of candidate molecules. The availability of PKPD relationships would also serve as the basis for the translation of the anti-nociceptive effects across species (1). In addition, the use of PKPD modelling offers an opportunity to better understand the *in vivo* time course of pharmacological effects, providing further insight into the mechanisms of action (13,14). Nonetheless, these concepts have been underutilised in pre-clinical pain research (15). This may be explained, at least partly, by the lack of pharmacokinetic information and the absence of the time course of treatment response (1).

The primary goal of this study was therefore to develop a semi-mechanistic model that allows the characterisation of the time course of formalin-induced pain and assess the effects of gabapentin on flinching behaviour. Above and beyond the known experimental issues, such as high variability in response, here we show that the main challenge for the characterisation of PKPD relationships using experimental behavioural pain models are the lack of suitable protocol designs, in which pharmacokinetic data and the time course of response are carefully considered. Lastly, we explore the relevance of parameter estimates by comparing our findings with published data from other experimental models of pain as well as with clinical data in neuropathic pain patients.

MATERIALS AND METHODS

Experimental Design

Protocols and experimental procedures were reviewed and approved by the Home Office, UK, as required per project licence. The experiments were performed following approval by the ethics Committee. Sprague-Dawley rats (Charles River, UK, weight range 100–300 g) had metal bands attached to their right hind-paws and were placed in Perspex recording chambers and allowed to habituate for 15 min before administration of formalin. The animals were then injected with 50 μl of formalin, subcutaneously in the ventral surface of the right hind-paw at a 2.5% conc/vol. Following formalin administration, animals were returned to the Perspex recording chambers and the number of flinches was counted by the automatic teller for 1 h. Four rats could be tested in parallel using this system. All animals were euthanised at the end of the experiment.

Vehicle or gabapentin was administered orally at doses of 0, 10, 30, 100 mg/kg approximately 1 h prior to formalin injection. The interval between drug administration and formalin injection is standard practice in the evaluation of analgesic drugs in this experimental model. It accounts for the time required for drug absorption and the short-lasting response to formalin (12). Data from five different experiments were pooled together, making a total of 96 animals. All experiments included a placebo or vehicle treatment arm, with eight animals per dose level. In four experiments only one active dose was tested (100 mg/kg), whilst the fifth experiment included two additional active doses levels of 10 and 30 mg/kg gabapentin.

Pharmacodynamic Measurements

The total frequency of flinches was recorded at 5-min intervals, from 5 to 60 min after formalin injection.

Data Analysis

Pharmacokinetic Simulations

Gabapentin concentrations were simulated using a model previously published based on a two-compartment drug disposition and dose-limited absorption (16). The model was built in a stepwise manner. First, intravenous data were modelled to

obtain accurate estimates of disposition parameters, namely clearance and volume of distribution. As gabapentin has poor solubility, nonlinear bioavailability is observed with increasing doses (17), absorption parameters (i.e., bioavailability and input rate) estimates were obtained separately from the fitting of a second experiment in which gabapentin was administered orally. Further diagnostics and validation procedures are described in Taneja *et al.* (16). Simulated gabapentin concentrations were derived by the following expression.

$$C = \frac{K_a FD}{V_1}\left\{\frac{(k_{21}-\lambda_1)e^{-\lambda_1 t}}{(k_a-\lambda_1)(\lambda_2-\lambda_1)} + \frac{(k_{21}-\lambda_2)e^{-\lambda_2 t}}{(k_a-\lambda_2)(\lambda_1-\lambda_2)} + \frac{(k_{21}-K_a)e^{-K_a t}}{(\lambda_1-k_a)(\lambda_2-k_a)}\right\} \quad (1)$$

where k_a = absorption rate constant, V_1 = central volume of distribution, F = bioavailability of the administered dose, λ_1 and λ_2 correspond to the initial and terminal slopes representing bi-exponential decline, respectively and k_{21} = micro-rate constant describing the transfer between compartments 1 and 2. A summary of the pharmacokinetic model parameters is shown in Table I. Details of the analytical solution to the two-compartment model, which was implemented in NONMEM for the simulations, and the derivation of the macro and micro rate constants from the primary pharmacokinetic parameters (i.e., volume and clearance) are described in the appendix (see Supplementary Material).

Exploratory Data Analysis

Before starting model building, we performed a graphical evaluation of the experimental data, including plots of the time course of gabapentin in plasma, the effect *vs.* time and the concentration *vs.* effect relationships. To ensure suitable model parameterisation and assess the existence of correlations in the data, pain response at any given point in time was also plotted against the values observed in the preceding interval. Such correlations are of relevance for modelling purposes, as highly correlated data may lead to model misspecification. In general, pain response (i.e., flinching frequency in our case) at a given sampling time has been shown to correlate with preceding measurements (18,19).

Given that the frequency of flinches/time interval was >10, we decided to model the counts as continuous data.

Table I Pharmacokinetic Parameter Estimates Used in the Simulations of Gabapentin Concentrations at the Time of Measurement of the Flinching Response

Pharmacokinetic parameter	Values
Central volume (V_1)	0.118 (l)
Peripheral volume (V_2)	0.253 (l)
Clearance (Cl)	0.159 (l/h)
Intercompartmental clearance(Q)	1.22 (l/h)
Bioavailability (F)	1,0.75,0.22[a]
Absorption rate constant (ka)	0.26 (h^{-1})

[a] For doses 10, 30,100 mg/kg respectively

PKPD Model Parameterisation

Disease Model. In the FIP model, there is a temporal delay between the appearance of gabapentin concentrations in plasma and the onset of the formalin-induced pain response. Depending on the half-life of the compound, the analgesic is administered before the induction of hyperalgesia with formalin. Given that two pain peaks consistently occur after administration of formalin, this phenomenon was parameterised in terms of two independent pharmacodynamic (PD) compartments. The first peak (i.e., pain associated with the first phase) was described by the following exponential decay relationship:

$$\frac{dFO}{dt} = -k_{df} * FO$$
$$PAIN_1 = F_3 * FO \quad (2)$$

where FO = formalin-induced stimulus, k_{df} = dissipation constant for formalin, F_3 = basal pain load in the first PD compartment, $PAIN_1$ = total pain in the first PD compartment

The first peak of pain occurs almost instantaneously after algogen administration, thus the parameter F_3 reflects pain at baseline, which wanes spontaneously soon thereafter.

The onset of the second peak of pain is after a quiescent phase and is considered to reflect the central hypersensitisation, which ultimately manifests itself as a second, more prolonged phase of flinching. Similarly to the first peak, pain intensity increases to a maximum and then remits spontaneously. Given the lack of a direct correlation between the gabapentin concentrations in plasma and the time course of this response over time, an indirect model was deemed to be most appropriate to describe the phenomenon (20). In an indirect model the measured response (R) is assumed to result from factors controlling either the input or the disappearance of the response. The general expression to describe these models is given by the expression below:

$$\frac{dR}{dt} = k_{syn} - k_{deg} * R \quad (3)$$

where dR/dt is the rate of change in the response over time, k_{syn} represents the zero-order rate constant for the formation of the response and k_{deg} the first-order rate constant for loss of the response. We have replaced the response R in Eq. 3 with the term FL to make explicit reference to the time course of

the flinching response triggered by the central sensitisation in the spinal cord following the first peak.

$$\frac{dFL}{dt} = k_{syn} - k_{deg} * FL \quad (4)$$

Given that the pain response wanes with time i.e., there is spontaneous recovery within 1 h after injection of the algogen (2,6), k_{syn} was treated as time-dependent variable and parameterised in conjunction with a lag time ($Tlag$). Depending on whether t, the time after formalin injection, was larger or smaller than $Tlag$ (i.e., the delay between the occurrence of the first and second peaks of pain), different estimates were considered for k_{syn}. Thus for $t \geq Tlag$, model parameterisation described the onset of the second phase of pain. If $t < Tlag$, $k_{syn} = 0$, which meant the second phase of pain had not yet begun. A modified gamma function was required to describe the time course of k_{syn} and Eq. 4 was thus transformed to an expression representing the natural change in pain frequency, as follows:

$$k_{syn} = A * \left(\alpha^{(t-Tlag)}\right) * e^{(-\beta(t-Tlag))} \quad (5)$$

where A (response unit h^{-2}), α (a dimensionless constant), β (h^{-1}) are the parameters of the gamma function describing the time course and intensity of the second phase of pain as assessed by the frequency of flinching.

As mentioned earlier, the time course of the disease is a result of the temporal change in the frequency of flinching represented by FL. At the start of the study, i.e., before onset of the second peak, the frequency of flinching was assumed to be 0. Consequently, the generic Eq. 4 can finally be rewritten in terms of FL as follows:

$$\frac{dFL}{dt} = A * \left(\alpha^{(t-Tlag)}\right) * e^{(-\beta(t-Tlag))} - k_{deg} * FL \quad (6)$$

Drug Model. The model used to describe the pharmacological effects of gabapentin was applied to simultaneously fit both placebo and active treatment data. It has been observed that gabapentin decreases the frequency of flinches, which results in a response profile superimposed on the natural disease process. Gabapentin effects *(DEFF)* were best described by an inhibitory I_{max} function, which represents the reversible counteracting effects of gabapentin on the algogenic action of FL, i.e., the observed flinching behaviour:

$$DEFF = \left(1 - \frac{I_{\max} * C_p}{IC_{50} + C_p}\right) \quad (7)$$

where I_{max} = maximum possible inhibition of pain, C_p = drug concentrations in plasma and IC_{50} = plasma concentration at which 50% of the maximum inhibition occurs. As gabapentin only affects the second peak of pain, we have assumed that gabapentin effects reflect a decrease in central sensitisation. We have assumed the I_{max} to be 1, i.e., the maximum possible inhibition of pain. This assumption is relevant from a drug development perspective, which implies complete pain suppression for truly effective treatments. In practice, however, one should acknowledge that current drugs do not appear to be completely efficacious. In addition, evoked pain in experimental models lead to different levels of hypersensitisation, which may result in varying peak intensities across different subjects (21).

From a modelling perspective, it should be noted that indirect response models incorporate the Hill function directly in the turnover differential equation whereas we have chosen to parameterise the gabapentin effect ($DEFF$) directly on the pain variable of the second peak, rather than within the differential equation. This is because gabapentin does not alter the onset of the pain nor its eventual disappearance, but reversibly alters its peak intensity. In other words, the analgesic effect of gabapentin is a covariate on the behaviour or flinching response. A similar approach has been used previously to describe the effects of lumiracoxib on COX-2 inhibition (22). The net pain observed is therefore the product of the gabapentin effect *(DEFF)* and FL. This effect has been parameterised into the second PD compartment *(PAIN2):*

$$PAIN2 = \left(1 - \frac{I_{\max} * C_p}{IC_{50} + C_p}\right) * FL \quad (8)$$

The total pain ($PAIN$) was described by the sum of the pain in the two PD compartments:

$$PAIN = PAIN1 + PAIN2 \quad (9)$$

A schematic representation of this mechanistic PD model is presented in Fig. 1. Interindividual variability was modelled exponentially and applied serially to each parameter. Stochastic parameters were retained in all cases in which significant improvements were observed to the fitting, as defined by statistical criteria described below. Residual variability was best described by an additive error model.

Model Diagnostics and Evaluation

Model selection was based on the visual examination of the goodness-of-fit plots using Xpose version 4.2.1 (23). The precision of model parameter estimates is represented by the coefficient of variation [CV (%)], computed as the ratio between the standard error provided by NONMEM and the parameter estimate multiplied by 100, and the MOFV provided by NONMEM. The difference in the MOFV between

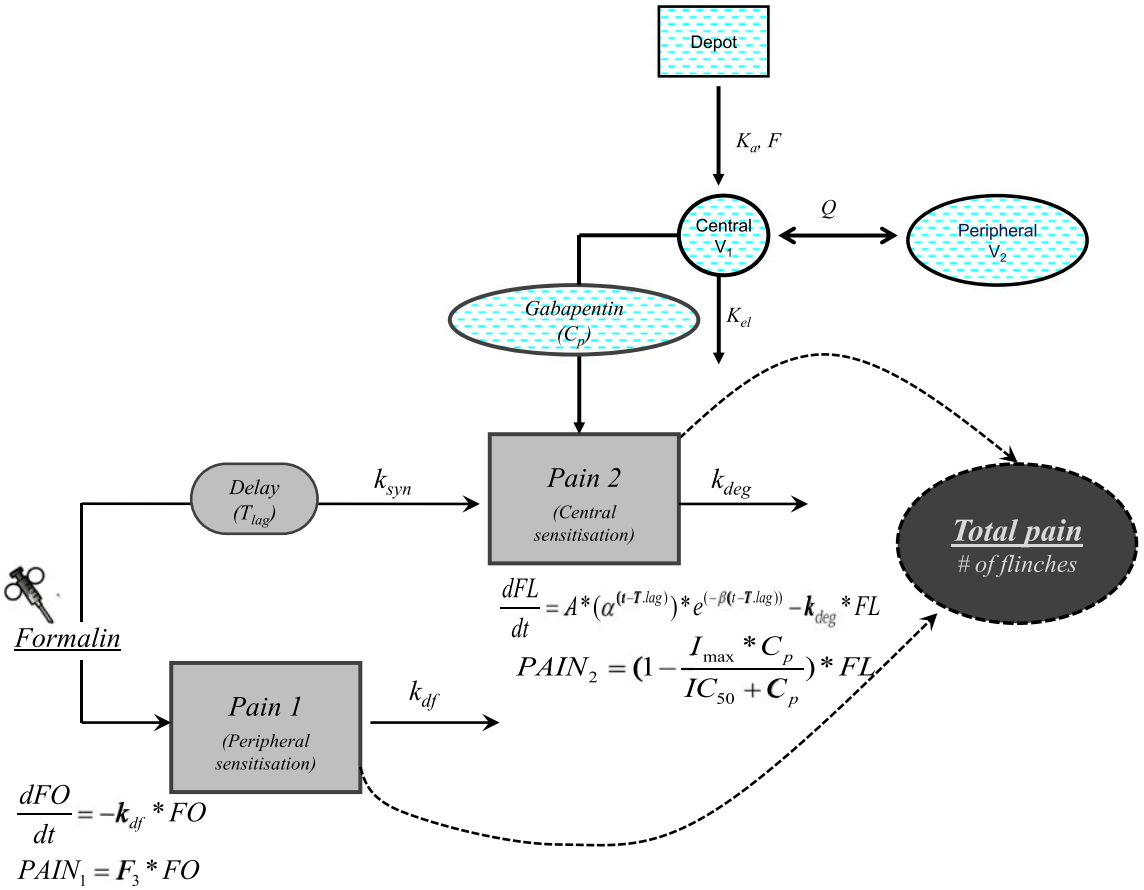

Fig. 1 Schematic diagram of the pharmacokinetic-pharmacodynamic model. PK compartments are displayed with *dashed horizontal* (*blue*) hatching, while PD compartments' are *dark shaded* (*grey* or *black*).

two hierarchical models was considered statistically significant if the MOFV changed by at least 6.63 points which is equivalent to a p value of <0.01 for a χ^2 distribution. The final model was further evaluated based on visual and numerical predictive checks and bootstrap procedures (24,25). Using the final model, the 2.5th, 50th, and 97.5th percentiles from simulated pain response ($n = 500$) were calculated and compared to the experimental data. NONMEM 7.1.2 was used in conjunction with PsN 3.2.12 for all estimation and simulation procedures. Modelling was based on the first-order conditional estimation method with the INTERACTION option (26). The statistical software R (v 2.10) was used for data manipulation, statistical and graphical summaries (27).

Lastly, a nonparametric bootstrap with re-sampling was performed to estimate the confidence intervals of the parameters (25). This technique consisted of repeatedly fitting the model to replicates of the data set using the bootstrap option in PsN 3.2.12. Parameter estimates for each of the replicate data sets were obtained. The results of successful runs from 500 bootstraps were then pooled together, and the median and 2.5th and 97.5th percentiles (denoting the 95% confidence interval) determined for each parameter.

RESULTS

Pharmacokinetic Simulations

The population mean concentration *vs.* time profiles for the three active doses of gabapentin are depicted in Fig. 2 (left panel). As indicated previously, drug concentrations increase less than proportionally with increasing doses due to the dose-limited bioavailability of gabapentin.

Exploratory Analysis

The time course of the flinching behaviour, summarised as means for each dose level is shown in Fig. 2 (right panel), together with the corresponding pharmacokinetic profiles. It can be appreciated here that gabapentin only reduces the amplitude of the second peak. Furthermore, the amplitude of the second peak decreases with increasing doses of gabapentin, highlighting a dose-dependent effect on flinching frequency.

Despite a dose-dependent effect on flinching frequency, Fig. 3 shows that there is a disconnection between the median behavioural response and population gabapentin

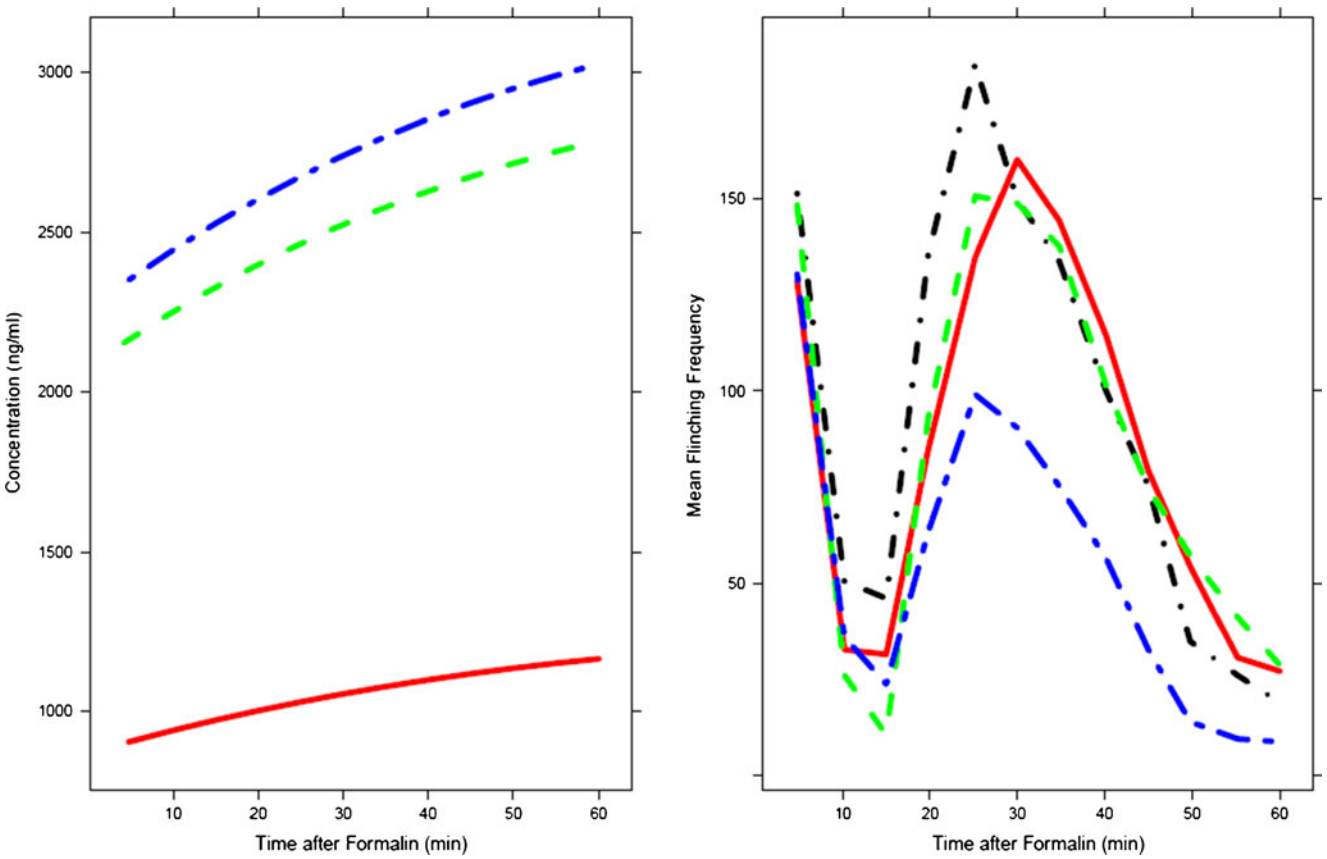

Fig. 2 Population curves for gabapentin concentrations in the plasma for doses 10, 30, 100 mg/kg (*left panel*) and the flinching behaviour in the formalin-induced model following placebo (*dot-dashed*), 10 (*solid*), 30 (*dashed*) and 100 (*dash-dash*) mg/kg curves (*right panel*).

concentrations. From these plots, it is clear that during the experimental protocol, the pain response (i.e., flinching frequency) begins soon after formalin injection and wanes while gabapentin is still predominantly in the absorption phase. Considerable variability in the response can also be seen between animals.

In Fig. 4, the flinching frequency is depicted against time and gabapentin concentrations, stratified by dose level. From the two panels it can be seen that the concentration-effect relationship can be superimposed on the time course of response itself. The data suggests that gabapentin effects have limited impact on the time course of the second pain peak. Moreover, this phenomenon is further confounded by high degree of correlation between consecutive measurements. Details are shown in the appendix (see Supplementary Material, Fig. S1).

PKPD Modelling

The time course of the flinching behaviour as well as the inhibitory effects observed after administration of gabapentin were accurately characterised by the indirect response model. The structural model described all three components of the pain response to formalin, namely the two peaks and the intervening quiescent phase between the peaks. The goodness-of-fit plots are presented in Fig. 5. All structural model parameters were identifiable for the current dataset, as evidenced from the RSEs (<40%) shown in Table II.

As can be seen from Figs. 3 and 4, there was considerable variability in the observed flinching frequency between different animals. IIV was modelled exponentially and tested serially on all model parameters. The data supported the inclusion of IIV on the F_3 parameter of the first peak, β, and k_{deg} on the second peak, resulting in significant drops in the objective function value i.e., yielding statistically significant improvements in the model ($p < 0.01$).

Model Evaluation

To evaluate model performance, the visual predictive checks were stratified by dose level. As can be seen in Fig. 6, the model is able to describe both the median trends in the data as well as the distribution i.e., the interquartile ranges. Since there was more data available for the placebo and 100 mg/kg dose, the predictions for these dose levels are comparatively better than for the remaining dose levels. Approximately, less than 5% of the observations fall outside the prediction intervals. The model predicted response for the second peak occurs slightly earlier than that of the real data, which may be due to

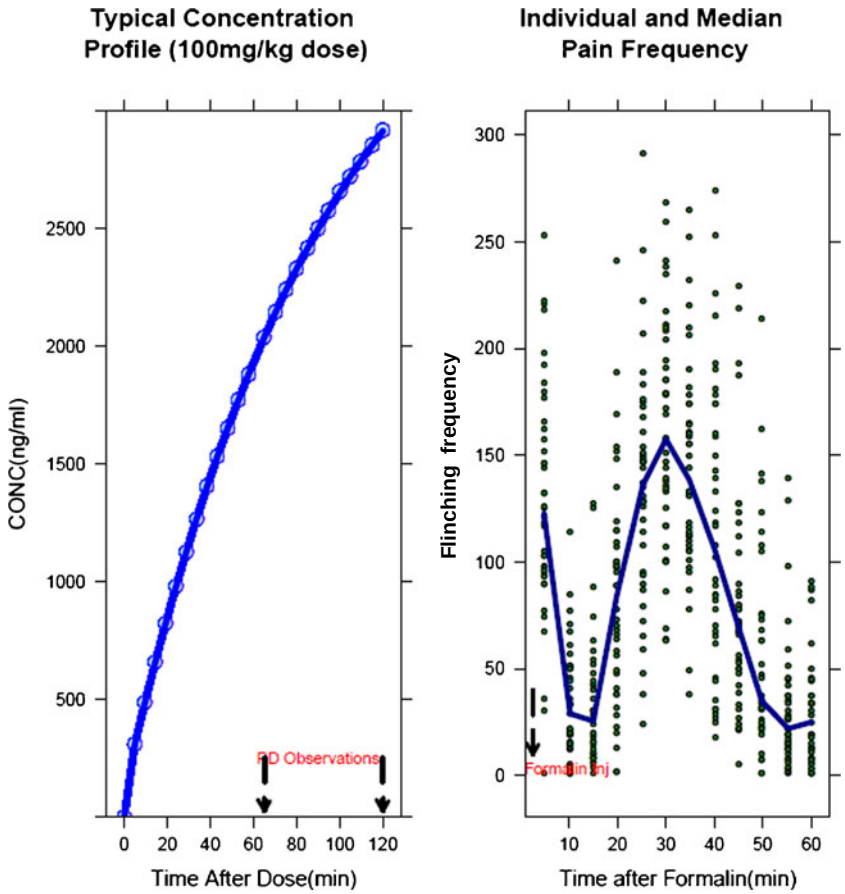

Fig. 3 Lack of correlation between the onset of response (*right panel*) and the time course of concentrations in plasma following a typical dose of 100 mg/kg gabapentin (*left panel*). *Dots* represent the individual observed flinching response expressed as counts/5 min; the *solid line* depicts the median response profile of the population in the study.

a slight underestimation of the lag time (T_{lag}). The numerical predictive checks are depicted in Table III, where the median number of flinching counts for observed and simulated (95% CI) data is shown at four different points, with the objective of characterising the maximum and minimum values of the two pain phases. In general, predictions for the placebo and

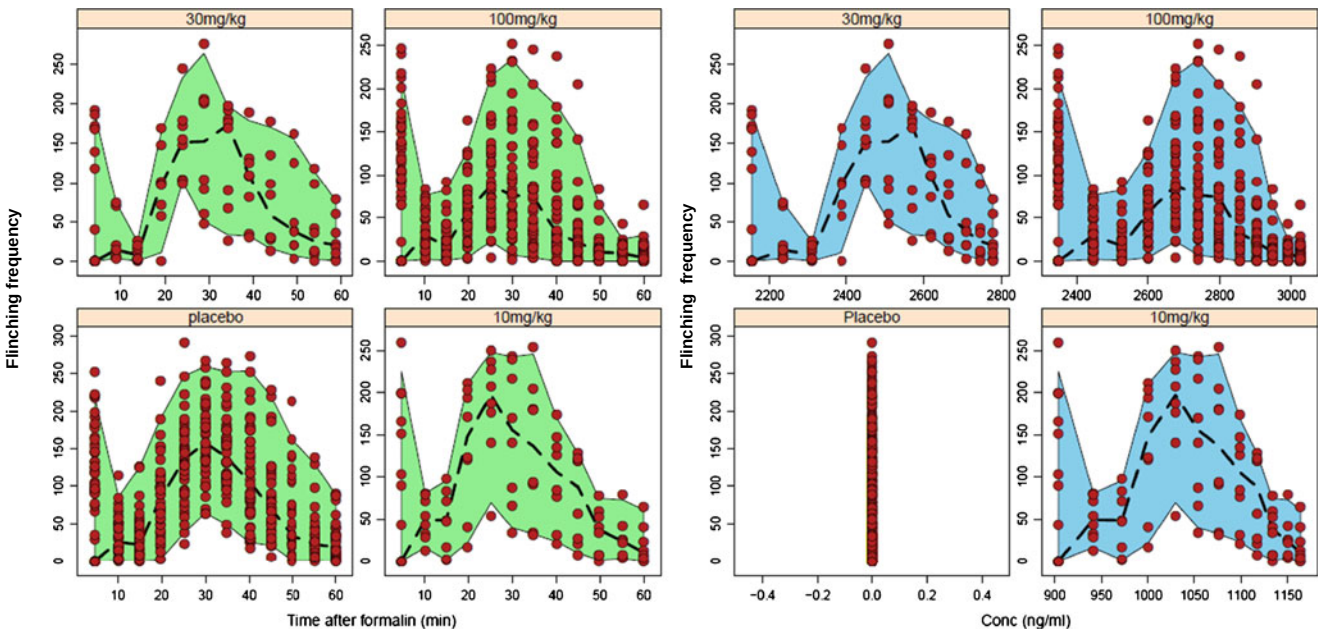

Fig. 4 Flinching frequency (expressed as counts/5 min) *versus* time and gabapentin concentration, stratified by dose level. The shaded area represents the 5th and 95th percentiles of the observed data.

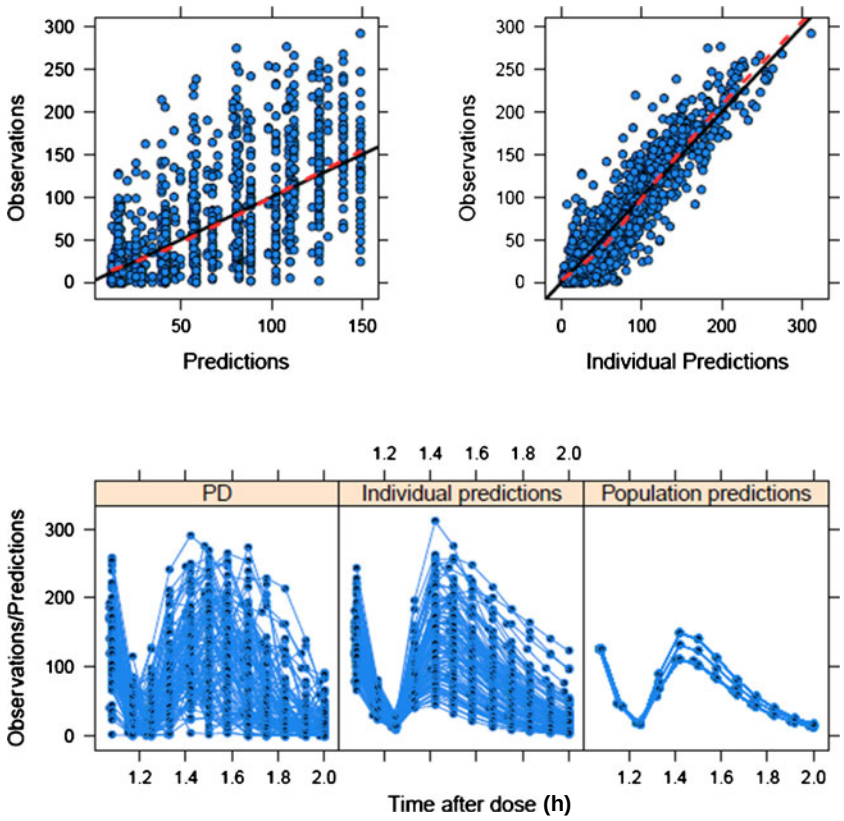

Fig. 5 Goodness-of-fit Plots. The *upper panels* show the correlation between observed and population (*left*) or individual (*right*) predicted response. In the lower panels, the observed and predicted responses are depicted over time.

100 mg/kg doses are better as compared to the other two, except in the case of the trough response for the second peak, where the model apparently seems to overpredict the frequency of counts, while underpredicting gabapentin effects, for the top dose as compared to the other dose levels. Such a discrepancy may be due to the effects of nonlinear bioavailability, which is not fully captured by imputed (simulated) concentrations. In fact, from Table III it can be seen that the predicted median maximal flinching frequency for the 100 mg/kg dose is less than the corresponding prediction for the 30 mg/kg dose and that the 95% CIs of the medians overlap with each other. This is a consequence of the actual concentrations of gabapentin driving the response, which did not differ widely across the dose levels.

Table II Parameter Estimates from the Final Population PKPD Model, Including Bootstrap Estimates and 95% Confidence Intervals

Final PD Model				Bootstrap Estimates			
				Parameter		IIV	
Parameter	Estimate (CV%)	IIV (CV%)	Shrinkage	Median	5%–95% CI	Median	5%–95% CI
k_{df} - constant for the dissipation of formalin effect (h^{-1})	12.3 (5.3)			249.3	12.33, 1169.25		
F_3 - basal response in the 1st PD compartment (*counts*)	126 (4.3)	57.4 (21.8)	16.7	132.0	122.32, 139.63	0.15	0.1, 34.6
Tlag – delay between the first and second peaks[a] (*h*)	0.3 (0.2)			0.24	0.0, 0.30		
A - parameter of gamma function (h^{-1})	2720 (6.6)	66.3 (17.0)	14.0	2275.8	1099.1, 2943.1	39.0	27.5, 46.8
α – dimensionless gamma function parameter	2.29 (239)			24.8	1.3, 159.0		
β – parameter of gamma function (h^{-1})	8.3 (30.8)	67.0 (78.0)	15.0	9.3	5.4, 12.1	25	7.2, 44.8
k_{deg} – degradation constant describing the waning of *Pain2* (h^{-1})	5.9 (4.2)			5.3	2.9, 6.3		
IC_{50} – gabapentin potency (*ng/ml*)	7510 (40.3)			6380.5	3961, 15390		
Residual error (additive)		29.1 (7.8)	9.4	35.3	33.0, 43.7		

IIV is presented as a percentage

[a] Tlag is relative to the formalin injection

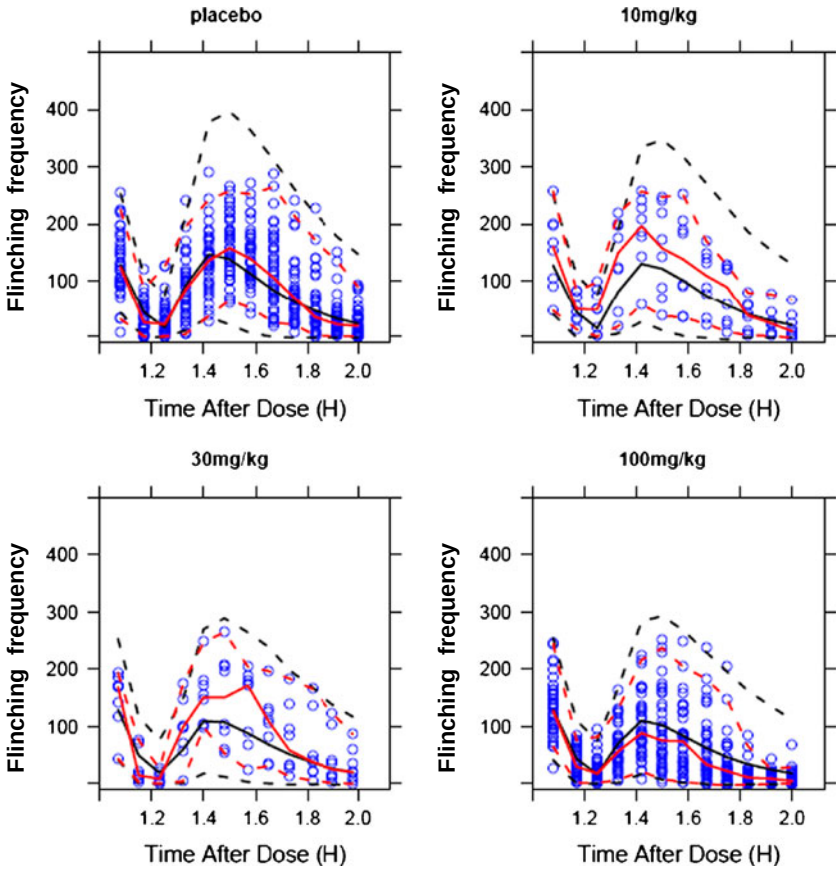

Fig. 6 Visual Predictive Check for the final PKPD model stratified by dose. The results are based on 500 replicates. *Filled Circles* are the raw data; the *red* and *black lines* denote the median of the observed and simulated data while the corresponding dashed lines represent the 2.5th and 97.5th percentile of the observed and simulated data respectively.

The final model parameter estimates along with the results from the bootstrap for 500 runs (median, 5 and 95% CI) is summarised in Table II. Most model parameters were well estimated, with the exception of k_{df}, α, and *Tlag* as can be seen from the wide confidence intervals in the bootstrap. Similarly, the parameters describing IIV were not well estimated in the bootstrap. We experienced a high minimisation failure rate in the bootstrap (~70%), which has caused a possible underestimation of IIV during bootstrapping. Therefore, all final IIV estimates are based on objective function criteria used during the initial fitting procedures. We do not consider these findings as a indication of model overparameterisation. Rather this suggests that not all parameters may be easily identifiable in subsets of the original dataset. The impact of poor precision was assessed by sensitivity analysis, which showed the variation in these parameters did not have significant effects on the overall model fit. Lastly, a few individual fits are depicted in Fig. 7 together with the observed data to illustrate model performance at the individual level.

DISCUSSION

Despite its wide use in the screening of compounds for neuropathic pain, till recently no attempts had been made to characterise PKPD relationships in the FIP model, with the

Table III Numeric Predictive Checks - Comparison Between Observed and Predicted Maximum and Trough Responses with Corresponding 95% Prediction Intervals Stratified by Dose

Dose (mg/kg)	Peak 1, Max PD (5 min after formalin injection)		Peak 1, Trough PD (10 min after formalin injection)		Peak 2, Max PD (30 min after formalin injection)		Peak 2, Trough PD (60 min after formalin)	
	Median Real data	Median Sim (95% CI)	Median Real data	Median Sim (95% CI)	Median Real data	Median Sim (95% CI)	Median Real data	Median Sim (95% CI)
0	123.1	128.1 (109.5–148.5)	22.1	16.4 (5.6–27.8)	157.4	137.8 (107.4–173.7)	19.1	23.4 (9.9–38.7)
10	159.6	126.9 (90.4–170.0)	48.0	14.9 (0.3–39.6)	157.0	121.0 (71.3–192.0)	9.7	21.6 (1.0–51.4)
30	169.1	130.0 (91.6–174.9)	8.1	18.5 (0.4–43.2)	171.5	87.9 (44.1–143.0)	19.7	19.6 (0.4–49.4)
100	126.5	128.5 (110.6–150.0)	17.5	16.2 (5.4–27.8)	75.0	102.0 (80.0–127.3)	4.4	17.7 (5.1–32.3)

exception of the recent work of Velez de Mendizabal *et al.* on lumiracoxib (22). Even though both investigations were based on FIP model, their approach is based on the use of a KPD (kinetic-pharmacodynamic) model to describe the effects of lumiracoxib. Their model shows that pain response during the second phase of the formalin-induced response can be described by incorporating synthesis and degradation of pain mediators that were recruited locally after tissue injury. Given the well-established role of COX-2, upregulation was correlated to predicted levels of pain mediators in the local (injured) compartment.

By contrast, the semi-mechanistic approach proposed here was aimed at the prospective use of PKPD models for drug screening. The model describes the time course of the disease (i.e., flinching frequency) and pharmacological effects (i.e., gabapentin) in an independent manner. In this context, gabapentin can be considered a paradigm compound. In addition, our choice of parameterisation took into account the possibility and importance of generating evidence of PKPD properties that can be easily used to translate treatment effects across species. Therefore, model parameterisation has not relied on typical measures such as cumulative response, which despite being technically less demanding has important drawbacks. For instance, if data were to be modelled using cumulative flinching counts, gabapentin potency would be expressed in terms of the time required to halve the maximum response. Such a parameter would have little physiological meaning even though many consider it suitable for ranking of compounds. Moreover, the use of such cumulative measures of response would not warrant a unique PKPD relationship (see Fig. 4). It became clear during our exploratory analysis that the flinching behaviour induced by formalin produces a unique fingerprint which prevails over any attempt to characterise the underlying exposure-response relationship using direct response models (28).

From a pathophysiological perspective, our efforts to parameterise the behavioural response enabled distinction between the first peak, i.e., peripheral sensitisation and the second peak, which appears to reflect central hypersensitisation. Furthermore, our approach clearly shows that it is possible to explore drug and disease properties using independent parameters. The drug-sensitive phase was therefore parameterised in terms of an indirect response model, which describes the changes in flinching behaviour in terms of the difference between a time-dependent synthesis and a constant degradation rate. The same phenomenon appears to occur in other species such as mice, gerbils, cats, monkeys (6), suggesting the opportunity for wide use of the concepts presented here. The formation rate of such a response (k_{syn}) was further characterised by a gamma function, which indicates the time varying course of formalin-induced symptoms, and consequently modifying the classical indirect response model of Dayaneka *et al.* (20). This function has been previously described for endpoints where spontaneous recovery from inflammation can be expected (14). Historically, negative power functions of time have been applied to describe clearance curves in PK studies

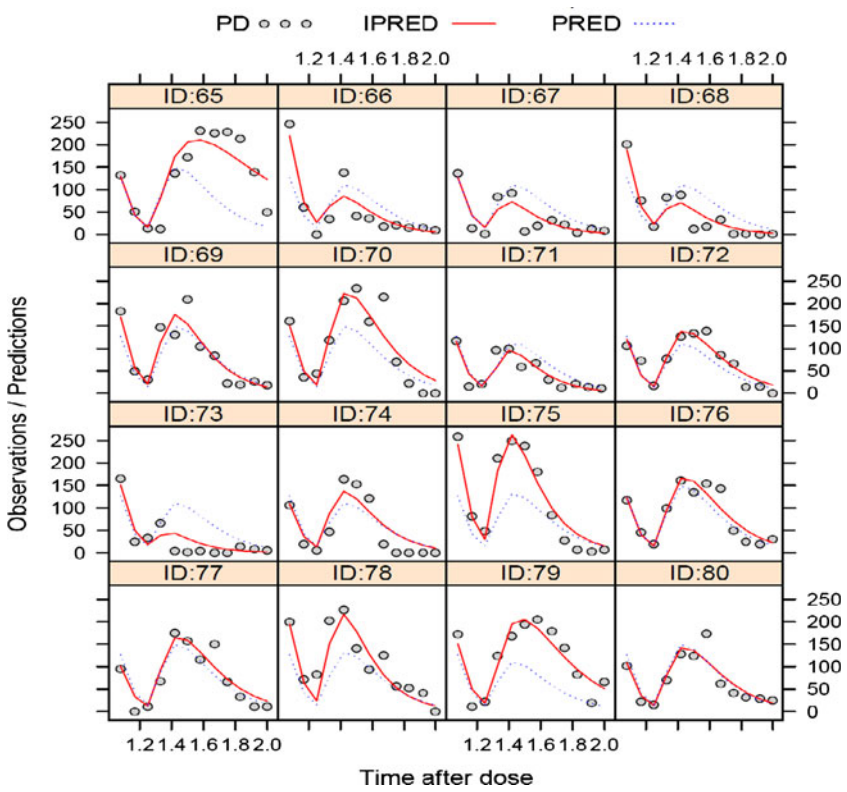

Fig. 7 Example of randomly selected observed individual profiles (*shaded circles*) with the corresponding individual (IPRED, *solid line*) and population predicted (PRED, *dotted line*) response.

and tracer kinetics in general, with a view to replacing multicompartmental analysis. Though non-physiological, they require considerably fewer parameters and yielded more accurate predictions (29). We have modified the traditional gamma function by parameterising the variable *t-Tlag* as the exponent of the dimensionless constant α. This led to better fits and lesser numerical difficulties with the minimisation routine. The time to onset of the second peak was about 20 min in our analysis which is in agreement with the observed data and also literature estimates of 10–20 min post-formalin injection (2). However, there was considerable variability in this parameter as can be seen from the median effect *vs*. time curves in Fig. 2. As indicated in the "Materials and Methods" section, we should mention that the assumption of a maximum drug response (I_{max}), with a theoretical value of 1 (i.e., return to a baseline state) allowed us to explore the concept of efficacy in a systematic manner. Fixing of the parameter to a single maximum value was applied even though the disease process and treatment response was not expected to be same in all subjects. The approach has been previously applied by Maas *et al.* to describe migraine pain (19).

Focus should also be given to the observed high between-subject variability in the FIP model, a phenomenon that is well known in clinical pain conditions (30,31). Although most investigations consider such variability a purely stochastic process which cannot be assigned to any specific source or mechanism, we have tried to estimate between-subject variability for all relevant model parameters, such as I_{max} or IC_{50}. Unfortunately, this was not supported by the data. Yet, it is reasonable to assume that individual differences in gabapentin potency do exist and occur due to the time varying effects of formalin, which can affect both maximum frequency of flinching behaviour as well as modulate gabapentin effects on central hypersensitisation. On the other hand, IIV could be identified for parameters associated with the induction of formalin-induced pain. The basal load of pain (F_3) differed among subjects and an η on this parameter improved the fit. The waning of the pain phenomenon (k_{deg}) was also found to differ among individuals and fitting showed significant improvements when IIV was applied. The diagnostic plots, such as the visual predictive checks show the model has adequate predictive performance. Ideally in such circumstances, the next step would be to fit the model to external datasets. Regretfully, we have not been able to identify such data.

Limitations

We should emphasise that the choice of parameterisation was based on turnover phenomena, rather than on disease states. In contrast to standard data-driven approaches in which variable states or grades of severity are parameterised as states in Markov-chain (32), we have chosen to handle the time course of flinching behaviour as a non-linear turnover process.

The identification of one or more states in such a fast waning process makes the estimation of transition probabilities in a hierarchical model rather challenging. In addition, flinching frequency data do not seem to support the concept of interchangeability in the transition between states, which is a desirable property of Markov processes. Interesting applications of hidden Markov models describing headache response after treatment with sumatriptan have been shown by Anisimov *et al.* and Maas *et al.* (19,33). Another example is the work published by Kjelsson *et al.*, where the authors describe how a Markov model can be used to describe sleep architecture (18). In either case, transition probabilities were used as basis for the evaluation of drug effects.

Another important point to consider is that complex pathophysiological processes underlie the generation of second peak, such as the release of various excitatory neurotransmitters acting through NMDA and NK1 receptors which then initiate a cascade leading to central sensitisation (34). We have parameterised these processes collectively as *FL*, under the assumption that differences in the individual time course of neurotransmitters was not statistically different. This choice was made to ensure description of the observed phenomenon rather than the pathophysiology of the pain response.

A potential drawback in our approach is that the IC_{50} estimates appear to be beyond the range of observed gabapentin concentrations. This situation is a consequence of the use of a theoretical maximum (I_{max}), which cannot be reached by gabapentin. Had this been the case, the second peak would have been suppressed completely. On the other hand, it is well documented that gabapentin produces partial symptomatic relief in neuropathic pain, rather than showing any disease modifying effects. It is therefore plausible to infer that incomplete suppression of the second peak reflects actual clinical effects of gabapentin (35,36). Yet, we consider the ability to discriminate between compounds that cause total pain suppression and partial relief highly desirable and do not anticipate any bias in the way compounds can be ranked on the basis of their potencies. In a situation where $C_p << IC_{50}$, the DEFF in Eq. 7 would reduce to:

$$DEFF = \left(1 - \frac{1}{IC_{50}}\right) \tag{10}$$

In this case, it can be argued that the IC_{50} would then be a linear coefficient rather than a true measure of potency and consequently yield a less robust estimate of the gabapentin effects. By contrast, under the assumption of a theoretical maximum response (I_{max}) being reached by an efficacious analgesic drug, the IC_{50} becomes a relative parameter, conditioned on I_{max} values. In these circumstances, IC_{50} estimates

can be reasonably used to compare compounds with each other as well as rank them according to differences in potency.

The identifiability of model parameters also deserves further discussion. We have not been able to identify all parameters with comparable precision, as can be seen from the results of the bootstrap procedures. This suggests the need for more frequent sampling schemes and larger datasets to fully characterise all model parameters. These findings are not necessarily a limitation. In fact, existing data may be used prospectively in future experimental protocols, in which the new data are used only to estimate compound-specific parameters and existing data continue to support the estimation of system-specific parameters. There are many recent examples in the published literature where this strategy has been employed. For the sake of conciseness, we refer the reader to these publications (37–39).

Finally, we acknowledge that the gamma function may have little physiologic basis, and future improvements to the model could be aimed at replacing this function with a more physiologic alternative. Such an alternative parameterisation may however require the availability of rich datasets. We anticipate that historical data may be used in combination with newly generated experimental data, so that only drug-specific parameters need to be estimated.

From a drug development perspective, we take the opportunity to highlight a few shortcomings of the experimental protocol design, which was performed according to standard experimental procedures. The time of dosing of gabapentin should have been planned taking into consideration differences in pharmacokinetic properties of the compounds under investigation. If gabapentin had been administered earlier, the return to baseline of the flinching events might have coincided with the elimination phase of gabapentin. Secondly, no baseline behaviour was recorded i.e., flinching counts between the administration of gabapentin and the injection of formalin ($T=0$). As explained previously, pain burden at baseline also showed differences between animals (i.e., interindividual variability on F_3).

Comparison with Other Pre-clinical and Clinical Findings

We have attempted to compare our results with other published pre-clinical and clinical data on gabapentin. Vastly different concentration levels have been reported in published preclinical gabapentin studies. These range from concentrations >5 μg/ml for oral doses ≥25 mg/kg (17) to values above 20 μg/ml at 2 h for oral dose of 30 mg/kg (40). These findings contrast with the simulated profiles that show gabapentin levels of approximately 2.5 μg/ml. These differences may result from high variability in absorption, which is mediated by active transporters (17). Furthermore, differences in drug metabolism may arise from wide range of body weights used in different publications. We also found differences in the relative bioavailability for the dose of 100 mg/kg. Our results suggest values of 22%, whilst Cundy *et al.* suggests bioavailability of approximately 50%. As described in the appendix, the pharmacokinetic model used for the simulations was based on oral data obtained by sparse sampling. The potential impact of sparse sampling on the estimates of bioavailability cannot be excluded. Further efforts are required to develop a more robust pharmacokinetic model for oral gabapentin using frequent sampling. However, one should remember that poor solubility and differences in the choice of solvents is also known to affect overall bioavailability.

Table S1 (see Supplementary Material) gives an overview of the IC_{50} and ID_{50} values reported for different pain models. Except for one pre-clinical experiment and one clinical study no other publications have applied modelling to analyse or interpret the data (41,42). Most authors used ID_{50}s and minimum effective doses (MED) as measures of potency with no mention of concentrations, rendering direct comparisons rather difficult, if not impossible (12,43–46). Noteworthy is the wide variability observed in the findings by different authors. There were other important differences such as the ceiling effect being observed by Iyengar *et al.* at a relatively low dose of 50 mg/kg, while others reported peak effects between 100–300 mg/kg (44,47). Among those studies where direct comparison with our work was possible, Todorovic reported an IC_{50} of 467 nM as compared to 43 nM reported here (41). More consistent results for clinical IC_{50}s were reported by Lockwood *et al.* (31.28 nM), whilst Whiteside *et al.* provide estimates for clinical MED values of 69.72 nM (42,48,49). Notably, Whiteside's work is the only effort at inter-species correlations amongst the publications we have reviewed, albeit not based on modelling concepts.

CONCLUSIONS

In summary, differences in analgesic potency exist in pre-clinical models, which cannot be interpreted simply in terms of precision. A comprehensive evaluation is missing of the differences and similarities in the underlying mechanisms affected by evoked pain in the various models currently available for pre-clinical evaluation of neuropathic pain.

Clearly, the challenges for the identification of suitable compounds for the treatment of neuropathic pain will not be overcome until adequate biomarkers of pharmacology are identified (50,51). Yet, irrespective of differences in pathophysiology, approaches are required that facilitate the translation of pre-clinical findings and provide the basis for the characterisation of drug-specific properties. A parametric, model-based approach is essential to ensure

distinction between disease processes and pharmacological effects.

ACKNOWLEDGMENTS AND DISCLOSURES

The authors acknowledge the contribution of Scott Marshall (Modelling & Simulation, Pfizer, Sandwich, UK), Ian Machin (Pain Research Unit, Sandwich, UK), and Dinesh DeAlwis (Global PK/PD/TS Europe, Eli Lilly, Erl Wood, UK), who have shared their experience with TIPharma and provided valuable insight into the issues faced by R&D during early drug development. Top Institute Pharma, a tripartite consortium involving industry, academia and the Netherlands government, has sponsored the PhD research programme of A. Taneja.

REFERENCES

1. Taneja A, Di Iorio VL, Danhof M, Della Pasqua O. Translation of drug effects from experimental models of neuropathic pain and analgesia to humans. Drug Discov Today. 2012;17:837–49.
2. Munro G, Erichsen HK, Mirza NR. Pharmacological comparison of anticonvulsant drugs in animal models of persistent pain and anxiety. Neuropharmacology. 2007;53:609–18.
3. Jarvisand MF, Boyce-Rustay JM. Neuropathic pain: models and mechanisms. Curr Pharm Des. 2009;15:1711–6.
4. Blackburn-Munro G. Pain-like behaviours in animals—how human are they? Trends Pharmacol Sci. 2004;25:299–305.
5. Le Bars D, Gozariu M, Cadden SW. Animal models of nociception. Pharmacol Rev. 2001;53:597–652.
6. Tjolsen A, Berge OG, Hunskaar S, Rosland JH, Hole K. The formalin test: an evaluation of the method. Pain. 1992;51:5–17.
7. Coderre TJ, Katz J, Vaccarino AL, Melzack R. Contribution of central neuroplasticity to pathological pain: review of clinical and experimental evidence. Pain. 1993;52:259–85.
8. Henry JL, Yashpal K, Pitcher GM, Coderre TJ. Physiological evidence that the 'interphase' in the formalin test is due to active inhibition. Pain. 1999;82:57–63.
9. Vissers KC, Geenen F, Biermans R, Meert TF. Pharmacological correlation between the formalin test and the neuropathic pain behavior in different species with chronic constriction injury. Pharmacol Biochem Behav. 2006;84:479–86.
10. Blackburn-Munro G, Ibsen N, Erichsen HK. A comparison of the anti-nociceptive effects of voltage-activated Na+channel blockers in the formalin test. Eur J Pharmacol. 2002;445:231–8.
11. Tanabe M, Ono K, Honda M, Ono H. Gabapentin and pregabalin ameliorate mechanical hypersensitivity after spinal cord injury in mice. Eur J Pharmacol. 2009;609:65–8.
12. Shannon HE, Eberle EL, Peters SC. Comparison of the effects of anticonvulsant drugs with diverse mechanisms of action in the formalin test in rats. Neuropharmacology. 2005;48:1012–20.
13. Vasquez-Bahena DA, Salazar-Morales UE, Ortiz MI, Castaneda-Hernandez G, Troconiz IF. Pharmacokinetic-pharmacodynamic modelling of the analgesic effects of lumiracoxib, a selective inhibitor of cyclooxygenase-2, in rats. Br J Pharmacol. 2010;159:176–87.
14. Giraudel JM, Diquelou A, Laroute V, Lees P, Toutain PL. Pharmacokinetic/pharmacodynamic modelling of NSAIDs in a model of reversible inflammation in the cat. Br J Pharmacol. 2005;146:642–53.
15. Martini C, Olofsen E, Yassen A, Aarts L, Dahan A. Pharmacokinetic-pharmacodynamic modeling in acute and chronic pain: an overview of the recent literature. Expert Rev Clin Pharmacol. 2011;4:719–28.
16. Taneja A, Nyberg J, de Lange EC, Danhof M, Della Pasqua O. Application of ED-optimality to screening experiments for analgesic compounds in an experimental model of neuropathic pain. J Pharmacokinet Pharmacodyn. 2012;39(6):673–81.
17. Cundy KC, Annamalai T, Bu L, De Vera J, Estrela J, Luo W, *et al*. XP13512 [(+/−)-1-([(alpha-isobutanoyloxyethoxy)carbonyl] aminomethyl)-1-cyclohexane acetic acid], a novel gabapentin prodrug: II. Improved oral bioavailability, dose proportionality, and colonic absorption compared with gabapentin in rats and monkeys. J Pharmacol Exp Ther. 2004;311:324–33.
18. Kjellsson MC, Ouellet D, Corrigan B, Karlsson MO. Modeling sleep data for a new drug in development using markov mixed-effects models. Pharm Res. 2011;28:2610–27.
19. Maas HJ, Danhof M, Della Pasqua OE. Prediction of headache response in migraine treatment. Cephalalgia. 2006;26:416–22.
20. Dayneka NL, Garg V, Jusko WJ. Comparison of four basic models of indirect pharmacodynamic responses. J Pharmacokinet Biopharm. 1993;21:457–78.
21. Lee DH, Chung K, Chung JM. Strain differences in adrenergic sensitivity of neuropathic pain behaviors in an experimental rat model. Neuroreport. 1997;8:3453–6.
22. Velez de Mendizabal N, Vasquez-Bahena D, Jimenez-Andrade JM, Ortiz MI, Castaneda-Hernandez G, Troconiz IF. Semi-mechanistic modeling of the interaction between the central and peripheral effects in the antinociceptive response to lumiracoxib in rats. AAPS J. 14:904–14.
23. Jonssonand EN, Karlsson MO. Xpose–an S-PLUS based population pharmacokinetic/pharmacodynamic model building aid for NONMEM. Comput Methods Programs Biomed. 1999;58:51–64.
24. Karlsson MO, Holford N. A tutorial on visual predictive checks, Population Approach Group of Europe Marseille France, 2008, p. 17 (2008=abtract 1434).
25. Ette EI, Williams PJ, Kim YH, Lane JR, Liu MJ, Capparelli EV. Model appropriateness and population pharmacokinetic modeling. J Clin Pharmacol. 2003;43:610–23.
26. Beal SL, Sheiner L. NONMEM users guides. In: Boeckmann TLA (ed.), Globomax ICON Development Solutions, Ellicott City,MD, 1989–2006.
27. R Development Core Team. R:A language and environment for statistical computing. In: R Foundation for Statistical Computing (ed.), Vienna Austria, 2011.
28. Uchizono JA, Lane J. Empirical pharmacokinetic/pharmacodynamic models. In: Ette E, editor. Pharmacometrics:the science of quantitative pharmacology. New Jersey: Wiley; 2007. p. 529–45.
29. Wise ME. Negative power functions of time in pharmacokinetics and their implications. J Pharmacokinet Biopharm. 1985;13:309–46.
30. Levy G. Predicting effective drug concentrations for individual patients. Determinants of pharmacodynamic variability. Clin Pharmacokinet. 1998;34:323–33.
31. Rahim-Williams B, Riley 3rd JL, Williams AK, Fillingim RB. A quantitative review of ethnic group differences in experimental pain response: do biology, psychology, and culture matter? Pain Med. 2012;13:522–40.
32. Newton PK, Mason J, Bethel K, Bazhenova LA, Nieva J, Kuhn P. A stochastic Markov chain model to describe lung cancer growth and metastasis. PLoS One. 2012;7:e34637.
33. Anisimov VV, Maas HJ, Danhof M, Della Pasqua O. Analysis of responses in migraine modelling using hidden Markov models. Stat Med. 2007;26:4163–78.
34. Yoonand MH, Yaksh TL. The effect of intrathecal gabapentin on pain behavior and hemodynamics on the formalin test in the rat. Anesth Analg. 1999;89:434–9.

35. Spallone V, Lacerenza M, Rossi A, Sicuteri R, Marchettini P. Painful diabetic polyneuropathy: approach to diagnosis and management. Clin J Pain.
36. Vorobeychik Y, Gordin V, Mao J, Chen L. Combination therapy for neuropathic pain: a review of current evidence. CNS Drugs. 25:1023–34.
37. Johnson M, Kozielska M, Pilla Reddy V, Vermeulen A, Li C, Grimwood S, *et al*. Mechanism-based pharmacokinetic-pharmacodynamic modeling of the dopamine D2 receptor occupancy of olanzapine in rats. Pharm Res. 2011;28:2490–504.
38. Taneja A, Nyberg J, Danhof M, Della Pasqua O. Optimised protocol design for the screening of analgesic compounds in neuropathic pain. J Pharmacokinet Pharmacodyn. 2012;39:661–71.
39. Milligan PA, Brown MJ, Marchant B, Martin SW, van der Graaf PH, Benson N, *et al*. Model-based drug development: a rational approach to efficiently accelerate drug development. Clin Pharmacol Ther. 2013;93:502–14.
40. Aryal B, Tae-Hyun K, Yoon-Gyoon K, Hyung-Gun K. A comparative study of the pharmacokinetics of traditional and automated dosing/blood sampling systems using gabapentin. Indian J Pharmacol. 2011;43:262–9.
41. Todorovic SM, Rastogi AJ, Jevtovic-Todorovic V. Potent analgesic effects of anticonvulsants on peripheral thermal nociception in rats. Br J Pharmacol. 2003;140:255–60.
42. Lockwood PA, Cook JA, Ewy WE, Mandema JW. The use of clinical trial simulation to support dose selection: application to development of a new treatment for chronic neuropathic pain. Pharm Res. 2003;20:1752–9.
43. Hamaand A, Sagen J. Behavioral characterization and effect of clinical drugs in a rat model of pain following spinal cord compression. Brain Res. 2007;1185:117–28.
44. Iyengar S, Webster AA, Hemrick-Luecke SK, Xu JY, Simmons RM. Efficacy of duloxetine, a potent and balanced serotonin-norepinephrine reuptake inhibitor in persistent pain models in rats. J Pharmacol Exp Ther. 2004;311:576–84.
45. Hurley RW, Chatterjea D, Rose Feng M, Taylor CP, Hammond DL. Gabapentin and pregabalin can interact synergistically with naproxen to produce antihyperalgesia. Anesthesiology. 2002;97:1263–73.
46. Yoonand MH, Yaksh TL. Evaluation of interaction between gabapentin and ibuprofen on the formalin test in rats. Anesthesiology. 1999;91:1006–13.
47. Yaksh TL. Spinal systems and pain processing: development of novel analgesic drugs with mechanistically defined models. Trends Pharmacol Sci. 1999;20:329–37.
48. Whiteside GT, Adedoyin A, Leventhal L. Predictive validity of animal pain models? A comparison of the pharmacokinetic-pharmacodynamic relationship for pain drugs in rats and humans. Neuropharmacology. 2008;54:767–75.
49. Whiteside GT, Harrison J, Boulet J, Mark L, Pearson M, Gottshall S, *et al*. Pharmacological characterisation of a rat model of incisional pain. Br J Pharmacol. 2004;141:85–91.
50. Huntjens DR, Danhof M, Della Pasqua OE. Pharmacokinetic-pharmacodynamic correlations and biomarkers in the development of COX-2 inhibitors. Rheumatology (Oxford). 2005;44:846–59.
51. Huntjens DR, Spalding DJ, Danhof M, Della Pasqua OE. Differences in the sensitivity of behavioural measures of pain to the selectivity of cyclo-oxygenase inhibitors. Eur J Pain. 2009;13:448–57.